A low-cost telerehabilitation paradigm for bimanual training

Roni Barak-Ventura, Manuel Ruiz-Marín, Oded Nov, Preeti Raghavan, Maurizio Porfiri, *Fellow, IEEE*

***Abstract*—The COVID-19 pandemic has transformed daily life, as individuals engage in social distancing to prevent the spread of the disease. Consequently, patients' access to outpatient rehabilitation care was curtailed and their prospect for recovery has been compromised. Telerehabilitation has the potential to provide these patients with equally-efficacious therapy in their homes. Using commercial gaming devices with embedded motion sensors, data on movement can be collected toward objective assessment of motor performance, followed by training and documentation of progress. Herein, we present a low-cost telerehabilitation system dedicated to bimanual exercise, wherein the healthy arm drives movements of the affected arm. In the proposed setting, a patient manipulates a dowel embedded with a sensor in front of a Microsoft Kinect sensor. In order to provide an engaging environment for the exercise, the dowel is interfaced with a personal computer, to serve as a controller. The patient's gestures are translated into interactive actions in a custom-made citizen-science project. Along with the system, we introduce an algorithm for classification of the bimanual movements, whose inner workings are detailed in terms of the procedures performed for dimensionality reduction, feature extraction, and movement classification. We demonstrate the feasibility of our system on eight healthy subjects, offering support to the validity of the algorithm. These preliminary findings set forth the development of precise motion analysis algorithms in affordable home-based rehabilitation.**

***Index Terms*—data science, inertial measurement unit, Microsoft Kinect, motion analysis, rehabilitation.**

I. Introduction

The COVID-19 pandemic has led to extraordinary paradigm shifts in healthcare systems worldwide. Human and material resources have been majorly reallocated for treatment of those stricken by the disease and non-urgent treatments have been suspended indefinitely [1]. Social distancing and other measures taken to minimize the spread of COVID-19 have further disrupted patients' access to healthcare services, negatively impacting their quality of life. For example, the number of stroke patients admitted for outpatient therapy plummeted by 50%-80%, suggesting that many patients who need rehabilitation care were not receiving it [2]. This state of emergency has highlighted the growing demand for telemedicine solutions that enable professionally-supervised home-based healthcare.

The most common cause of post-stroke disability is hemiparesis, or weakness on one side of the body, which limits limb mobility and encumbers the performance of daily activities. Consequently, many stroke survivors experience reduced functional independence and require costly caregiving. In order to recover muscle strength and regain self-reliance, stroke survivors must adhere to a rehabilitation regimen consisting of frequent high-intensity exercises [3], [4]. In particular, rehabilitation during the first six months post-stroke has been shown to be crucial for optimal recovery. Within this period, stroke survivors achieve the greatest improvements in upper limb function, ambulation, and speech [5], [6], [7]. Therefore, preserving access to rehabilitation care at the beginning of the regimen is especially important for stroke rehabilitation outcomes.

The need for a stroke telerehabilitation framework was recognized over twenty years ago, when advancements in information technologies made the notion of telerehabilitation realizable [8], [9]. One of the first examples of a web-based telerehabilitation system was presented in 2002 by Reinkensmeyer et al. [10]. Java Therapy consists of a haptic joystick interfaced with a series of recreational exercises that quantify movement toward remote assessment of coordination and motor control. Altogether, the system trains shoulder internal rotation along with shoulder and elbow flexion. Another telerehabilitation system, InMotion2 (the commercial version of the MIT Manus robot), can operate interactively where the patient can train cooperatively with a therapist or with another patient online [11]. This robot aims to rehabilitate shoulder and elbow movements and can target the wrist joint and fingers upon coupling with dedicated modules [12], [13]. Similarly, teleAutoCITE is a tabletop workstation affixed with an array of tools for training of functional manual tasks [14]. Sensors embedded in the tools measure the user's performance, and a camera and a personal computer enable videoconferencing with a therapist. The system provides constraint-induced therapy whereby exercise is performed with the affected limb while the unaffected limb is constrained.

In contrast, bimanual training emerged as an effective clinical approach for the recovery of coordinated movements using both hands whereby the intact limb facilitates movement of the paretic limb [15]. In spite of its proven effectiveness, few examples of bimanual training exist in telerehabilitation of upper limb movement. Empirical evidence shows that bimanual training helps reacquire voluntary motion in paretic limbs through several physiological mechanisms. Passive movement of an impaired limb could impart "overflow" of electrical impulses to the affected muscles, thereby promoting muscle activity and strength [16], [17]. Similarly, neural pathways underlying bilateral movements may project to regions of the primary motor cortex contralateral to the unaffected limb and increase the likelihood of voluntary movement in the impaired limb [18], [19]. Bimanual training is also advantageous for practical reasons: bimanual skills are more abundant in activities of daily living and relearning how to use both hands cooperatively will help patients regain their independence more quickly [20].

Here, we present a low-cost telerehabilitation system dedicated to bimanual training. The system consists of a Microsoft Kinect sensor, and a wooden dowel embedded with an inertial measurement unit

R. Barak-Ventura and M. Porfiri are with the Department of Mechanical and Aerospace Engineering, New York University Tandon School of Engineering, Brooklyn, New York 11201, USA.

O. Nov is with the Department of Technology Management and Innovation, New York University Tandon School of Engineering, Brooklyn, New York 11201, USA.

P. Raghavan is with the Department of Physical Medicine and Rehabilitation, Johns Hopkins School of Medicine, Baltimore, Maryland 21218, USA

M. Ruiz-Marín and M. Porfiri are with the Department of Quantitative Methods, Law and Modern Languages, Technical University of Cartagena, 30201, Cartagena, Murcia, Spain

M. Ruiz-Marín is also with Murcia Bio-Health Institute (IMIB-Arrixaca), Health Science Campus, 30120, Cartagena, Murcia, Spain

M. Porfiri is also with the Center for Urban Science and Progress and the Department of Biomedical Engineering, New York University Tandon School of Engineering, Brooklyn, New York 11201, USA. E-mail: mporfiri@nyu.edu (corresponding author)

Manuscript received <Month> <day>, 2020; revised <Month> <day>, 2020

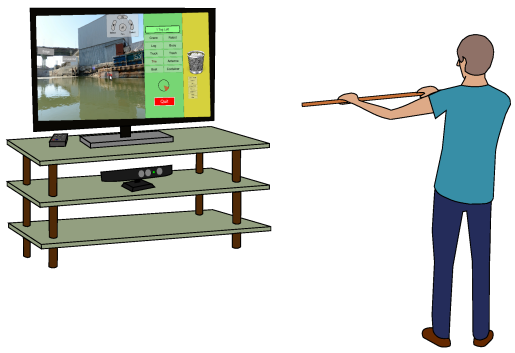

Fig. 1: Set-up of the proposed system, integrated with a citizen-science project. The user holds the dowel with both hands and manipulates it in space to control an application that is launched on a monitor (a custom-made citizen science project, in this case). A Kinect sensor is positioned below the monitor and records the user's movements.

(IMU). The Microsoft Kinect is a commercial entertainment device that enables a natural user interface by means of skeleton tracking. The Kinect records the position of 15 joints in three dimensions, without the need for markers [21], [22]. Its precision was evaluated in several studies and the device was found suitable for objective analysis of human motion in rehabilitation [23]. Our proposed system implements a natural user interface in which the user manipulates the dowel while facing the Kinect (Figure 1). By fusion of data collected through the Kinect and the IMU, intuitive input gestures with the dowel translate into actions on a computer screen. In this manner, the dowel can serve as a controller for a wide variety of serious games [24].

Although often overlooked, the manner in which rehabilitation exercises are presented to patients is essential to their rehabilitation outcomes. Framing the exercise in an intrinsically motivating context can inspire patients to adhere to their rehabilitation program [25], [26]. Thus, our system enables the user to participate in a custom-made citizen science project. Specifically, the user analyzes 360° images of a polluted canal, taken by a robotic boat that monitors the quality of water [27], [28]. Pre-defined bimanual gestures allow the user to explore the picture, move the cursor, and click buttons. Hence, the role of the Kinect in our system is twofold. First, it provides information on the user's posture and movement to assess the quality of motion during exercise. Second, it relays control commands based on body gestures that it captures, enabling an engaging natural user interface.

In conjunction with the physical system, we propose the application of a movement classification algorithm, which is a considerable component of our system's novelty. The algorithm is used to classify the movements the user performs toward a genuine telerehabilitation practice, where one's motor performance can be truly assessed by a therapist remotely. Such an automatic classification of movements is expected to reduce the amount of time and effort practitioners spend inspecting and interpreting kinematic data. In addition, as the algorithm records data continuously throughout a regimen, it could provide objective assessment of the rehabilitation progress as classification becomes more distinct.

Automatic classification of movements in telerehabilitation is still underdeveloped. Past studies have applied principles from data science for motion analysis in rehabilitation medicine, however, the vast majority of this research focused on lower limbs. Early work on recognition of gait patterns utilized neural networks [29] and fuzzy clustering techniques [30]. These methods were soon replaced by hidden Markov chains, which became the exemplary approach for gait detection and classification [31], [32], [33]. Machine learning was utilized in this domain as well. For example, Begg and Kamuzzaman [34] used a support vector machine classifier to uncover the kinematic underpinnings of falls among the elderly. Similarly, Novak et al. used a support vector machine algorithm to identify phases of gait at different speeds [35]. For rehabilitation of the upper limbs, statistical pattern recognition algorithms were used to quantify motor performance of the upper limb from data collected by vision-based sensors [36] or inertial sensors [37]. Apart from that, data-driven algorithms remain underutilized in the assessment of upper limb movement, and completely unutilized in the evaluation of bimanual movements.

Herein, we present a simple, yet effective, data-driven algorithm to automatically assess bimanual movements. The algorithm implements dimensionality reduction, followed by an ensemble classifier. The algorithm automates the classification of movement with high accuracy and could ultimately reduce the time and cost of post-stroke rehabilitation assessment by a therapist.

II. Prototype Design

The low-cost system consists of a Microsoft Xbox 360 Kinect sensor (Microsoft Corporation, Redmond, Washington) and a $3/4$ inch diameter standard wooden dowel. A custom-made cubic box is 3D printed and installed at the center of the dowel. The box houses an IMU (MPU-6050, InvenSense Inc., Sunnyvale, California), an Arduino Nano microcontroller (Arduino, Italy), and HC-05 Bluetooth module to transmit the IMU recordings in real time. The IMU is fixed in the box such that when the box is placed on a flat surface and the dowel is horizontal, its x-axis is perpendicular to the ground, the z-axis is perpendicular to the dowel and parallel to the ground, and the y-axis is parallel to the dowel (Figure 2).

Although the Kinect can record motion with sufficient accuracy for application in rehabilitation [23], it has certain limitations [38]. Primarily, when joints are occluded, the Kinect estimates a skeleton model and introduces noise and errors into the measurements [39]. In our system, a user may hold the dowel and flex their shoulders to 90°, thereby occluding the Kinect's view of the elbow and shoulder joints with their hands. In such a case, the Kinect may erroneously interject elbow flexion and shoulder abduction ([39]; Figure 3). To overcome this issue, the simultaneous use of multiple Kinect sensors has been proposed [40]. The use of multiple Kinect sensors simultaneously in a home setting comes with a few limitations. For example, multiple devices would require a larger space, as the distance of a user from the sensor needs to be a minimum of four feet. For these practical

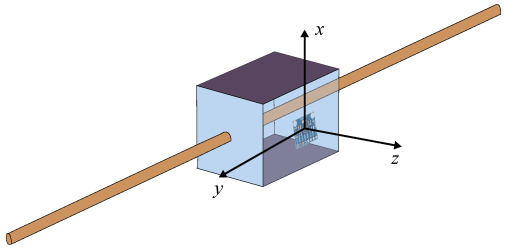

Fig. 2: Orientation of the IMU when fixed to the dowel, at the baseline pose. The y-axis is parallel to the dowel and the z-axis extends perpendicular to it, parallel to the ground. The x-axis completes an orthogonal coordinate system.

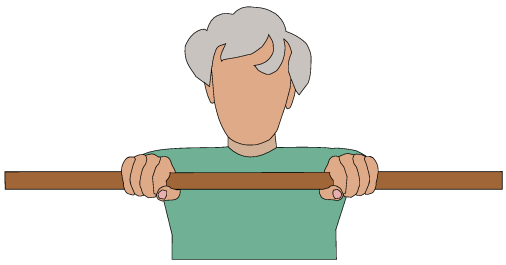

Fig. 3: The user from the Kinect's point of view. When the user keeps their elbows straight and flexes their shoulders, the hands could occlude the Kinect's view of the elbows and shoulders. As a result, the Kinect will estimate these joints' positions and introduce an error into the measurement.

reasons and in the interest of maintaining a low cost, we chose to incorporate an IMU into the system.

The Kinect is used for assessment of motor performance as well as for implementation of a natural user interface, whereby bimanual manipulation of a dowel in front of the sensor would translate to in-game functions. An environmental citizen science project is displayed, where the user explores 360° images of a polluted canal, selects labels, and allocates them onto objects of interest such as potential pollutants and notable landmarks. If the user aims to move the cursor on the screen to the left, they should abduct their left shoulder and adduct the right shoulder, moving the dowel to the left while keeping it parallel to the ground (Figure 4a). Similarly, to move the cursor to the right, the user should perform shoulder adduction and abduction in the opposite direction, moving the dowel to the right while maintaining it horizontal (Figure 4a). To move the cursor upward, the user should flex both shoulders and lift the dowel (Figure 4b). To move the cursor downward, the user should extend both shoulders and lower the dowel (Figure 4b). To explore the 360° images, the user should tilt the dowel clockwise or counterclockwise to turn left or right (Figure 4c), and flex or extend their wrists (Figure 4d) to look up or down. Finally, to select a label or allocate it, the user should flex and then extend their elbows, pushing the dowel away from their body along the transverse plane (Figure 4e).

The proposed movements employ most joints of the upper limbs and are commonly prescribed for home-based rehabilitation [41], [42]. Typically, stroke patients tend to not use their affected limb and reinforce maladaptive, non-physiological movements [43]. Learnt non-use impedes recovery and perpetuates disability [44]. Thus, it is of high interest to promote motion of the limb, whether it is moved actively or passively [45]. The support of bimanual exercise by a dowel can be beneficial for reducing compensatory movements, as well as for recovering the affected arm's passive range of motion [46].

The natural user interface implementation was achieved with a simple fuzzy logic scheme so that in-game response would not lag. Specifically, the fuzzy logic scheme was applied with respect to the relative position of joints. For example, the cursor would move to the left if the left elbow's position relative to the left shoulder's position along the x-axis exceeded a certain threshold, and simultaneously, the right elbow's position relative to the right shoulder's position along the x-axis exceeded a different threshold. The thresholds were determined in a calibration phase, where the user was instructed to move their arms to the extents of their range of motion. In this manner, the system's responsiveness to the user's movements could be adapted to accommodate for a compromised range of motion.

III. Data collection

To demonstrate our system, we collected data on healthy subjects who interacted with the system. The study was conducted in compliance with the guidelines and regulations set forth by New York University's institutional review board, the University Committee on Activities Involving Human Subjects (UCAIHS; IRB FY2019-2828).

Eight subjects were recruited (three female and five male; average age of 24.1 $\pm$ 4.6). Each subject was escorted to a private room where they were introduced to the project and the system. The Kinect sensor was re-positioned and its angle was adjusted between experiments to strain the developed approach and assess its robustness to unavoidable variations in real-world applications.

The experiment began with calibration to measure the subject's range of motion and adjust the system's sensitivity to their movements. First, the subject performed horizontal shoulder abduction. Starting from a baseline pose with their arms held straight and parallel to the ground, they first performed horizontal shoulder abduction toward their left side and returned to the center, repeating this movement five times. Then, the subject performed horizontal shoulder abduction to the right and returned to the center five times. In the same manner, the subject performed shoulder flexion and extension, rotated the dowel counterclockwise and clockwise parallel to the coronal plane, performed wrist flexion and extension, and performed elbow flexion and extension, in this order. The subject repeated each movement five times consecutively and returned to the original position after each excursion. A video illustrating the calibration is available in the supplementary material.

After calibration, the subject completed a five-minute tutorial which taught them how to use the dowel as a controller. Then, they analyzed images of a polluted canal for as long as they wished. When the subject quit the application, they filled out a short questionnaire, assessing the intuitiveness of the interface, its ease of use, and the engaging nature of the citizen science activity.

Three data sets were generated during this exercise for each subject. The first data set was produced by the Kinect and logged the subject's joint positions in three dimensions. The second data set comprised the IMU measurements and recorded its Tait-Bryan angles (yaw about the z-axis, α; pitch about the y-axis, β; and roll about the x-axis, γ), rotational velocities (ω_x, ω_y, and ω_z), and gravitational acceleration along the axes (g_x, g_y, and g_z), obtained through the built-in function dmpGetGravity available on MPU-6050. These two data sets were collected synchronously at a sampling rate of 18 measurements per second. The third data set contained the subjects' responses to the questionnaire.

The data sets were processed in MATLAB (MATLAB R2020a, The MathWorks, Inc., Natick, Massachusetts, United States). Given the three-dimensional position of each joint from the Kinect, a skeleton model of the user's body was reconstructed. We defined the reference frame with its origin fixed at the shoulder-center joint ([47], [48]; Figure 5). The X-axis was parallel to the ground and the Y-axis was perpendicular to the ground. Both axes lay in the plane containing the left and right shoulder joints. The Z-axis was orthogonal to this plane, following the right-hand rule. The vectors that corresponded to limb segments were computed by subtraction of the coordinates of a joint at one end of the limb from the coordinates of the joint at the other end of the limb.

For each time step, four instantaneous joint angles were computed for each arm: shoulder horizontal abduction ($\theta_{1,\mathrm{L}}$ and $\theta_{1,\mathrm{R}}$), shoulder flexion ($\theta_{2,\mathrm{L}}$ and $\theta_{2,\mathrm{R}}$), wrist flexion ($\theta_{3,\mathrm{L}}$ and $\theta_{3,\mathrm{R}}$), and elbow flexion ($\theta_{4,\mathrm{L}}$ and $\theta_{4,\mathrm{R}}$), where L and R denote the left and right

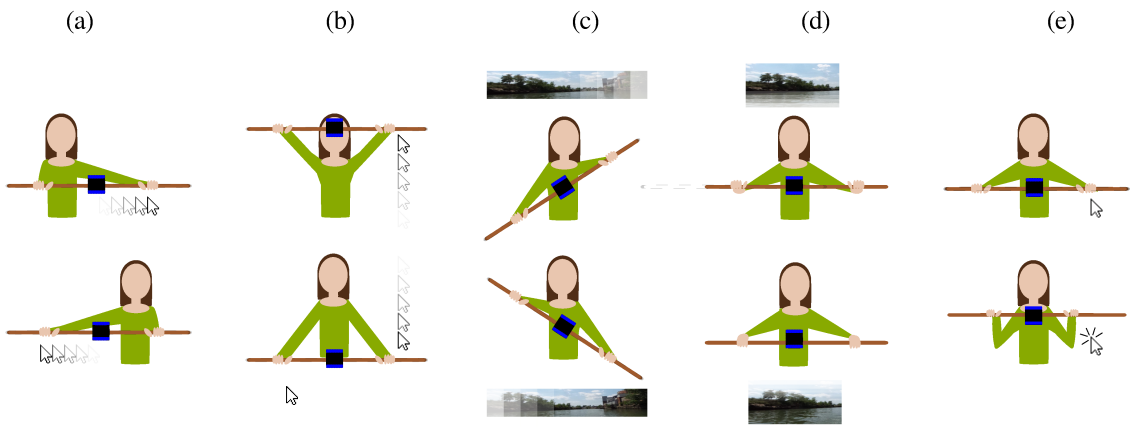

Fig. 4: Illustration of the movements implemented in the natural user interface. The user is able to perform actions on a computer through (a) horizontal abduction and adduction of the shoulders (moving the cursor left or right), (b) flexion and extension of the shoulders (moving the cursor up or down), (c) rotation of the dowel clockwise and counterclockwise (rotating the image left or right), (d) flexion and extension of the wrists (rotating the image up or down), or (e) flexion and extension of the elbows (selection of objects). The blue square represents the 3D-printed cube that contains the IMU and electronic circuits.

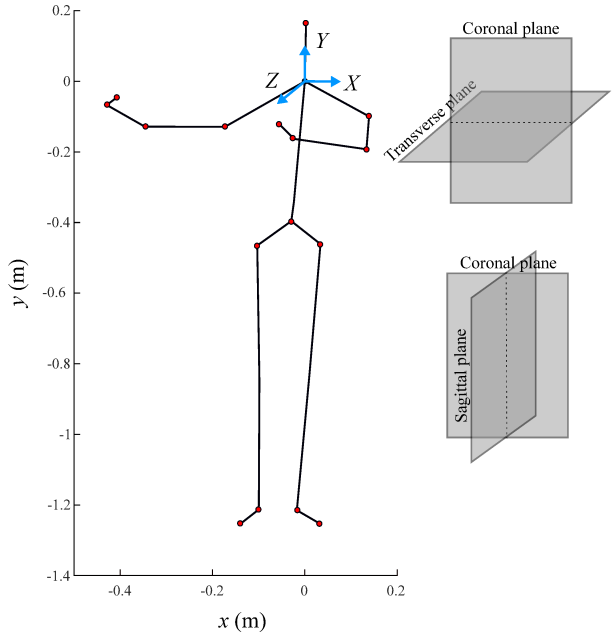

Fig. 5: Schematic of the skeleton model constructed from Kinect data, while the subject performed shoulder abduction. The black lines represent segments and the red circles represent the 20 articular joints between them. The reference frame is placed at the neck, colored in blue. The X-Y, X-Z, and Y-Z planes correspond to the coronal, transverse, and sagittal planes, respectively.

arms, respectively. Instantaneous shoulder abduction angles were inferred by projecting the model's arm onto the transverse plane and computing the angle it formed relative to the ground through the inverse tangent (Figure 6a). Similarly, shoulder flexion angles were computed from projection of the model's arm onto the sagittal plane through the inverse tangent (Figure 6b). Elbow angles were computed using the scalar product between the model's arm and forearm. Since grasp of the dowel blocked the wrist from the Kinect's view, wrist

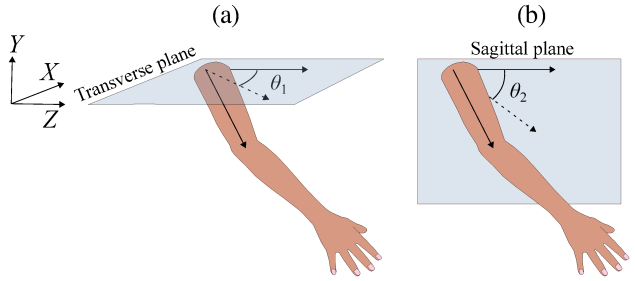

Fig. 6: Illustration of computation of (a) shoulder abduction angle (θ_1) and (b) shoulder flexion angle (θ_2). The dashed line represents the projection of the arm's vector onto the transverse and the sagittal planes (depicted with grey rectangles) to form angles θ_1 and θ_2 with a vector that is parallel to the ground, respectively.

flexion angles were inferred from the IMU pitch measurements. A third-order median filter was applied to remove noise. Data points above and below the top and bottom percentiles were removed. For added insight on the kinematics of movements, instantaneous angular velocities for each joint movement ($\dot{\theta}_{1,\mathrm{L}}$, $\dot{\theta}_{1,\mathrm{R}}$, $\dot{\theta}_{2,\mathrm{L}}$, $\dot{\theta}_{2,\mathrm{R}}$, $\dot{\theta}_{3,\mathrm{L}}$, $\dot{\theta}_{3,\mathrm{R}}$, $\dot{\theta}_{4,\mathrm{L}}$, and $\dot{\theta}_{4,\mathrm{R}}$) were computed by applying a central difference scheme on angle measurements. Overall, the time series of 25 variables were considered in the analysis (Table I).

IV. Motion Analysis

In the analysis, we focused on the calibration phase, where the movements subjects performed were known. We aimed to classify these movements using the measurements captured by the Kinect and the IMU through a data-driven methodology. Our approach unfolded along three distinct steps: principal components analysis (PCA), feature extraction, and movement classification via a bagged tree algorithm.

A. Principal components analysis

As a first step, we identified the salient variables which characterize each movement among the available 25 variables through PCA (Figure 7a). Time series were visually inspected to identify segments

of movement and the type of movement performed. To standardize the selection of segment boundaries and avoid false identification of noise as movement, segments where defined as instances where IMU rotational velocity exceeded 2 $\mathrm{deg/s}$.

Within segment k, the time series of each of the 25 variables was normalized with respect to its own standard deviation throughout the segment; We use $\tilde{(\cdot)}$ to denote the normalized time series. The normalized time series were used to create a covariance matrix for segment k, denoted U^k (Figure 7b), that is,

$$U^k_{ij} = (\tilde{u}^k_i - \bar{\tilde{u}}^k_i)^{\mathrm{T}} (\tilde{u}^k_j - \bar{\tilde{u}}^k_j) \tag{1}$$

where $i,j = 1, 2, ..., 25$; 1, 2, ..., 25, and $\bar{\tilde{u}}$ is the average value of the time series of variable $\tilde{u}$.

The principal components of covariance matrix U^k were given by the eigenvectors $\boldsymbol{\nu}^k_n$ associated with its largest eigenvalues λ^k_n,

$$U^k \boldsymbol{\nu}^k_n = \lambda^k_n \boldsymbol{\nu}^k_n, \tag{2}$$

with $n = 1, \ldots, N^k_{PCA}$ where N^k_{PCA} is the number of eigenpairs (eigenvalues and corresponding eigenvectors) that were retained for further analysis. To pinpoint the dominant eigenvalues, a spectral gap was identified as the largest difference between consecutive eigenvalues sorted in a descending order (Figure 7c). N^k_{PCA} was taken as the number of eigenvalues that preceded the gap, which typically was equal to 1.

Once the dominant eigenvalues have been identified, we explored the role of their corresponding eigenvectors. We sorted the absolute values of the components of each eigenvector in a descending order and defined a gap as the largest difference between consecutive values. We retained for analysis the components of the eigenvector that appeared before the gap (Figure 7d). In principle, the number of components that preceded the gap could vary between subjects, since individuals move very differently from one another.

Once the components were identified for all segments in all subjects, we determined the most common components. Focusing on one movement type at a time, we aggregated the principal components from all segments and all subjects and kept a count of the number of times each was observed (Figure 7e). We then selected two components, one for each arm, to describe bimanual movements. For example, 261 components were aggregated from all subjects for horizontal shoulder abduction to the left. The most common component in the right arm was $\theta_{1,R}$ (observed 32 times) and the most common component in the left arm was $\theta_{1,L}$ (observed 31 times). Therefore, those components were deemed principal for left horizontal shoulder abduction. In the case where the most salient variables were associated with the IMU on the dowel, we retained only one of them toward a minimalistic representation of the movements.

Results of the PCA are summarized in Table II. We found that shoulder abduction in either direction is characterized by changes in $\theta_{1,\mathrm{L}}$ and $\theta_{1,\mathrm{R}}$. Shoulder flexion and extension were strongly associated with changes in $\theta_{2,\mathrm{R}}$ and $\theta_{2,\mathrm{L}}$. As expected, variations in α were predominant in the vertical rotation of the dowel in either direction. Wrist flexion was characterized by variation in β. Finally, elbow flexion was characterized by appreciable changes in $\theta_{3,\mathrm{R}}$ and $\theta_{3,\mathrm{L}}$.

Sensor	Variable	Observation	Notation
Microsoft Kinect	u_1	right shoulder abduction angle	$\theta_{1,\mathrm{R}}$
	u_2	right shoulder flexion angle	$\theta_{2,\mathrm{R}}$
	u_3	right elbow flexion angle	$\theta_{3,\mathrm{R}}$
	u_4	right wrist flexion angle	$\theta_{4,\mathrm{R}}$
	u_5	left shoulder abduction angle	$\theta_{1,\mathrm{L}}$
	u_6	left shoulder flexion angle	$\theta_{2,\mathrm{L}}$
	u_7	left elbow flexion angle	$\theta_{3,\mathrm{L}}$
	u_8	left wrist flexion angle	$\theta_{4,\mathrm{L}}$
	u_9	right shoulder abduction velocity	$\dot{\theta}_{1,\mathrm{R}}$
	u_{10}	right shoulder flexion velocity	$\dot{\theta}_{2,\mathrm{R}}$
	u_{11}	right elbow flexion velocity	$\dot{\theta}_{3,\mathrm{R}}$
	u_{12}	right wrist flexion velocity	$\dot{\theta}_{4,\mathrm{R}}$
	u_{13}	left shoulder abduction velocity	$\dot{\theta}_{1,\mathrm{L}}$
	u_{14}	left shoulder flexion velocity	$\dot{\theta}_{2,\mathrm{L}}$
	u_{15}	left elbow flexion velocity	$\dot{\theta}_{3,\mathrm{L}}$
	u_{16}	left wrist flexion velocity	$\dot{\theta}_{4,\mathrm{L}}$
IMU	u_{17}	roll angle	γ
	u_{18}	pitch angle	β
	u_{19}	yaw angle	α
	u_{20}	rotational velocity about u-axis	ω_x
	u_{21}	rotational velocity about y-axis	ω_y
	u_{22}	rotational velocity about z-axis	ω_y
	u_{23}	gravitational acceleration along x-axis	g_x
	u_{24}	gravitational acceleration along y-axis	g_y
	u_{25}	gravitational acceleration along z-axis	g_z

TABLE I: Summary
of the variables collected by the Microsoft Kinect and inertial measurement unit. A subscript L or R indicates the left or right arm.

Movement Performed	Associated Variables
Shoulder abduction (left)	$\theta_{1,\mathrm{R}}, \theta_{1,\mathrm{L}}$
Shoulder abduction (right)	$\theta_{1,\mathrm{R}}, \theta_{1,\mathrm{L}}$
Shoulder flexion	$\theta_{2,\mathrm{R}}, \theta_{2,\mathrm{L}}$
Shoulder extension	$\theta_{2,\mathrm{R}}, \theta_{2,\mathrm{L}}$
Vertical rotation (counterclockwise)	α
Vertical rotation (clockwise)	α
Wrist flexion	β
Wrist extension	β
Elbow flexion	$\theta_{3,\mathrm{R}}, \theta_{3,\mathrm{L}}$

TABLE II: Summary
of the PCA results. The number of prominent variables is determined based on the relative size of the eigenvector's components.

B. *Feature extraction*

The PCA informed us of the salient variables in each movement. Variables carrying the highest value explained the majority of variance and therefore contained the most information in each movement. We used these characteristic variables to create discriminating statistics, which would serve as the features to train the classification algorithm with. Given knowledge of the movement that was performed, the algorithm would explore different relationships between the features that distinguish one movement from another [49].

Importantly, we observed that the eigenvector components associated with α were prominent during clockwise and counterclockwise vertical rotation. Similarly, β was prominent during wrist flexion and extension. These variables may be uniquely characteristic for the aforementioned movements, and therefore, their ranges were selected to serve as features. The remaining movements performed in this study were associated with changes in horizontal shoulder abduction, shoulder flexion and extension, or elbow flexion angles. The ranges for these six variables were also selected to serve as features, reaching a total of eight range values.

To distinguish between the movements with a few features that encapsulate in part these combinations, we chose to use correlation coefficients, relating two variables at a time as additional features. We considered the correlations between each of the joints with their counterparts in the other arm ($\theta_{1,R}$ and $\theta_{1,L}$, $\theta_{2,R}$ and $\theta_{1,L}$, and $\theta_{3,R}$ and $\theta_{3,L}$). We also assessed the correlations between ipsilateral and

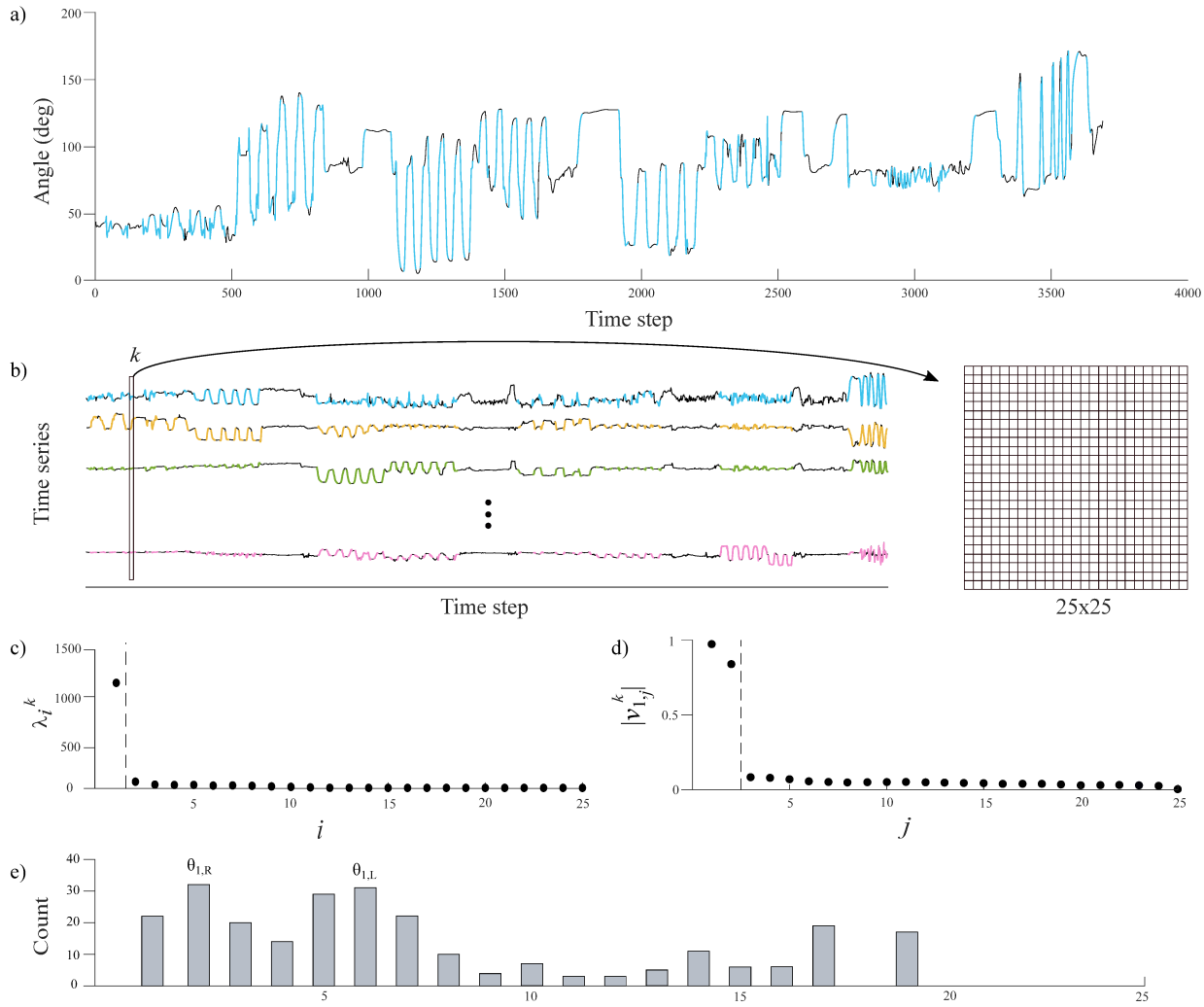

Fig. 7: Schematic of the PCA process. First, segments where a movement takes place are identified. An examplary time series of right shoulder flexion angle for one of the subjects (Subject 8) is displayed in (a). The blue segments in the time series were identified as instances of movements, corresponding to the nine different movements the subject performed sequentially (five times each): shoulder abduction to the left, shoulder abduction to the right, shoulder flexion upward, shoulder extension downward, counterclockwise vertical rotation, clockwise vertical rotation, wrist flexion upward, wrist extension downward, and elbow flexion, respectively. For a time segment k, the time series of each of the 25 variables are used to generate a 25×25 covariance matrix. In (b), a segment where horizontal shoulder abduction to the left was performed is selected in a box and the covariance matrix is computed. The spectrum of the covariance matrix is used to infer N_{PCA}^k, the number of eigenvalues that were retained in the analysis. In (c), only one eigenvalue, λ_1^k, precedes the gap (reflected with a dashed line). The components of ν_1^k are plotted in (d), which indicates that only two components in this eigenvector are important, corresponding to variables u_1 and u_5 ($\theta_{1,\mathrm{R}}$ and $\theta_{1,\mathrm{L}}$). After the same process is carried out for all segments of wrist flexion in all subjects, the important components of eigenvectors are aggregated, as seen in (e). The two variables that are most common across subjects are then identified ($\theta_{1,\mathrm{R}}$ and $\theta_{1,\mathrm{L}}$, in this case) and used to devise features.

contralateral horizontal shoulder abduction and shoulder flexion angles ($\theta_{1,R}$ and $\theta_{2,L}$, $\theta_{1,L}$ and $\theta_{2,R}$, $\theta_{1,R}$ and $\theta_{2,R}$, and $\theta_{1,L}$ and $\theta_{2,L}$). For a complete representation of the IMU data, the correlation between β and α was added to the analysis, thereby resulting in a total of eight correlation coefficients to be included alongside the eight range values.

We applied the algorithm using a moving window, such that we evaluated the 16 selected features within a window of several time steps, shifted the window by a time step, evaluated the features again, and so on. In this manner, the evolution of the features can be explored in future endeavors with pathological movements. The short duration of certain movements (that is, wrist flexion had an average duration of 1.1 seconds) raised concerns that the window could contain more than a single movement. Therefore, the length of the moving window was limited to 15 time steps, equivalent to 0.83 seconds. This duration guaranteed that the moving window would not contain more than a single movement, yet was sufficiently long for distinguishable computation of the selected features.

In order to apply a supervised machine-learning technique, a robust classification must be defined for each window, and labeled with the corresponding movement performed. We visually inspected the time series and identified which movement was performed (if any) at each time step. Then, as the window moved one step at a time, we classified it based on the mode movement of the time steps it contained. That is, the window's true class matched the class of the majority of time steps.

C. Movement classification

We used the Classification Learner app on MATLAB to train the algorithm. We entered the frames' true classes and the features associated with them as the training data set and included all 15 features as predictors. We opted for K-fold cross-validation specifying $K=5$, and selected ensemble classifier Bagged Trees for the model type.

Bagged Trees emerged as a method of choice to overcome the high variance of classification trees by means of bootstrapping and aggregation [50], [51]. Briefly, through this algorithm, a multitude of decision trees are generated by re-sampling the data set with replacement. The majority vote of their predictions (the mode classification) is recorded as the predicted response class. One of the advantages of using Bagged Trees is the possibility of scoring the importance of each feature in the classification process by estimating "out-of-bag" error. In this approach, the instances that were not sampled when a tree was generated are used to make a prediction. The mean prediction error of this "out-of-bag" sample is computed and the variables which produce the minimum error are considered the most important ones.

Classification was performed for features aggregated across subjects, as well as for each subject individually. Our model reached an accuracy of 93.1%. The true positive rate (TPR) was highest for elbow flexion, reaching 92.9% success in classification (Table III). The algorithm was least favored in classification of shoulder abduction to the right and shoulder extension, where TPR reached 85.4%. The majority of false negatives (66.5% of all false negatives and 4.5% of all observations) resulted from classification of movements as non-movements.

Out-of-bag analysis showed that the ranges of β and $\theta_{1,L}$ were critical in the classification of movements (Figure 8). Among the correlation coefficients, the one between $\theta_{1,L}$ and $\theta_{1,R}$ was most important. The remaining correlations between joint angles and their counterparts in the other arm were scored least important. Among the ranges, $\theta_{3,R}$ contributed the least to classification.

Subject-specific results for the classification are summarized in Table IV. For each subject, we report the accuracy of the classification and the TPR for each movement. As expected, the classifier's performance in Table III was similar to the mean of its performance on individual subjects in Table IV. The standard deviations extended from 1.1% to 6.3%, suggesting robustness with respect to inter-subject variability. The standard deviation was lowest for identification of a static pose (1.1%) and then for counterclockwise vertical rotation (2.2%). It was highest for wrist flexion (6.3%) followed by shoulder abduction to the right and shoulder extension (5.7% for both). Interestingly, even though the first author (Subject 1) had the most experience with the system, the performance of the algorithm on her data was virtually indistinguishable from others.

The classifier's accuracy for individual subjects was generally higher than 93.1%, with the exception of Subject 6 and Subject 8, who reached 90.5% and 92.9% accuracy, respectively. In particular, these subjects had the lowest TPR values for the majority of movements: shoulder abduction to the left, shoulder abduction to the right, shoulder extension, counterclockwise vertical rotation, and wrist extension.

V. Usability and Engagement

Subjects completed a questionnaire assessing the usability of the system and their enjoyment from interacting with it. Specifically, subjects were asked to score the extent to which they agree with the following statements, on a 7-point Likert scale: "The platform was intuitive to use", "I learned easily how to use the platform", and "I enjoyed the activity". The responses from Subject 1, the first author, were excluded from the analysis. On average, subjects easily learned how to use the system (5.7 ± 1.1; mean $\pm$ standard deviation) and found that it was intuitive to use (4.8 ± 0.7). The subjects also enjoyed the activity and rated it as 5.1 ± 0.9.

VI. Discussion

The COVID-19 pandemic has placed unprecedented strain on healthcare systems across the globe. In efforts to mitigate the spread of the virus among healthy populations, in-person medical services have been heavily restricted. Among the patients who were affected by the COVID-19 decrees are stroke survivors with hemiparesis, who require long term outpatient rehabilitation to regain muscle strength, motor skill, and self-reliance. It has been known for several decades that access to rehabilitation care is critically important for recovery from stroke, yet, the unusual circumstances of COVID-19 accentuate this issue. To meet the rising demand for affordable and accessible telerehabilitation, we developed a novel low-cost system for telerehabilitation of stroke-induced disability. The system mediates bimanual training, such that the intact limb aids movement of the paretic limb. A Kinect sensor would track the patient's skeleton and an IMU would record the dowel's orientation, toward objective assessment of motor performance.

The data drawn from these sensors is used for implementation of a natural user interface, enabling the user to participate in engaging activities while performing bimanual movements. Bimanual training is proven to effectively recover voluntary movements among hemiparetic patients. It offers physiological and practical advantages, and it is commonly prescribed for home-based rehabilitation [41], [42]. Our system serves as one of the first examples for low-cost telerehabilitation systems that employ this clinical approach. The interface we created translates the user's bimanual gestures to actions in an environmental citizen science project. Specifically, the user is able to analyze images of a polluted canal and help scientists map important landmarks in its area [27], [28]. This approach capitalizes on human intellect as an intrinsic motivator, and adds a sense of accomplishment and empowerment to the actions performed, thereby enhancing adherence to the rehabilitation regimen.

Importantly, we supplemented our system with a robust data science-principled classification algorithm. Automating classification of human movements represents another step toward a genuine telerehabilitation paradigm, where sensor data that is sent to practitioners is already processed and analyzed. The algorithm classified bimanual movements objectively and reliably, reaching 93.1% accuracy. Notably, the 6.8% inaccuracy does not stem from misclassification of movements as other movements but rather from lack of sensitivity with respect to the existence of a movement. That is, inaccuracy was majorly caused by classification of movements as instances of no movement. For example, out of 1,936 instances of shoulder abduction to the right, 275 were classified as no movement, and only seven were erroneously misclassified as shoulder abduction to the left or shoulder extension. Such an imperfect sensitivity likely emerged from our use of a moving window scheme in the algorithm training. Specifically, the true class of a window was defined by the mode of the true classes it covered. At the beginning and ending of each movement, it is tenable that time steps' true classes within the window were marginally divided (that is, eight time steps belonged to one class and seven time steps belonged to another class). Classifying the window as one of two classes introduces some arbitrariness into the training. Therefore, the accuracy of our approach may be further improved by refining this scheme and eliminating false negatives.

Reaching an accuracy of 93.1% offers compelling evidence in favor of our approach. Notably, the position and angle of the Kinect

True class \ Predicted class	No movement	Shoulder abduction (right)	Shoulder abduction (left)	Shoulder flexion	Shoulder extension	Vertical rotation (counterclockwise)	Vertical rotation (clockwise)	Wrist flexion	Wrist extension	Elbow flexion
No movement	17642 (96.7%)	81 (0.4%)	61 (0.3%)	90 (0.5%)	64 (0.4%)	58 (0.3%)	78 (0.4%)	57 0.3%)	33 (0.2%)	86 (0.5%)
Shoulder abduction (right)	275 (14.2%)	1654 (85.4%)	6 (0.3%)		1 (0.1%)					
Shoulder abduction (left)	201 (11.4%)	12 (0.7%)	1548 (87.9%)							
Shoulder flexion	150 (9.5%)			1410 (89.8%)	11 (0.7%)					
Shoulder extension	214 (13.2%)			16 (1.0%)	1388 (85.4%)	2 (0.1%)		1 (0.1%)		5 (0.3%)
Vertical rotation (counterclockwise)	126 (10.7%)		2 (0.2%)		1 (0.1%)	1047 (88.5%)	5 (0.4%)	2 (0.2%)		
Vertical rotation (clockwise)	127 (10.0%)				1 (0.1%)	2 (0.2%)	1128 (89.1%)	3 (0.2%)	5 (0.4%)	
Wrist flexion	167 (14.3%)							995 (85.5%)	2 (0.2%)	
Wrist extension	67 (8.6%)							10 (1.3%)	699 (90.1%)	
Elbow flexion	68 (6.6%)		2 (0.2%)		4 (0.4%)					964 (92.9%)

TABLE III: Table of confusion summarizing the success of the classification algorithm on all the subjects. Each row summarizes classification for one movement whereby it breaks down classes to which its instances were assigned. For example, shoulder abduction to the right side of the body was accurately identified as such in 1,654 of 1,936 instances. Thus, the TPR with respect to this movement is 85.4%. Across all movements, 28,499 out of 30,571 instances were classified correctly, such that the algorithm reached a TPR of 93.1%.

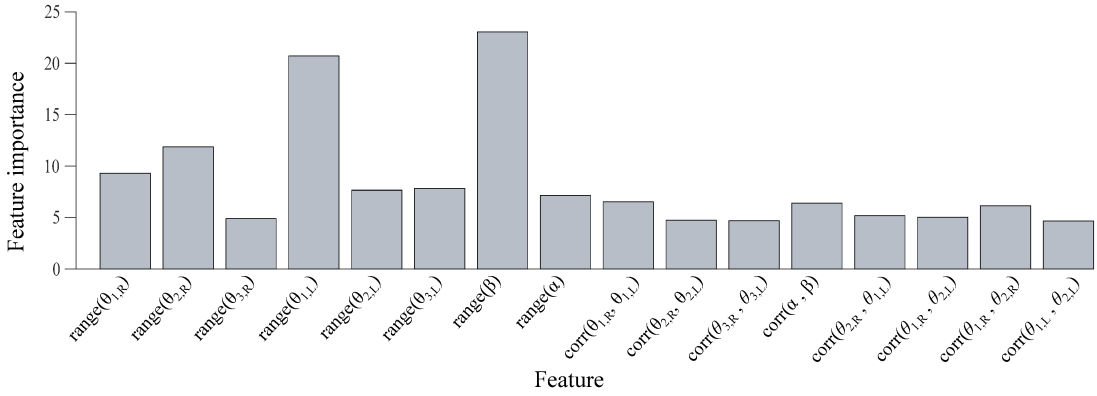

Fig. 8: Feature importance based on "out-of-bag" error estimation.

Subject	Accuracy	No movement	Shoulder abduction (right)	Shoulder abduction (left)	Shoulder flexion	Shoulder extension	Vertical rotation (counterclockwise)	Vertical rotation (clockwise)	Wrist flexion	Wrist extension	Elbow flexion
1	94.4%	96.9%	87.9%	93.7%	93.4%	81.8%	89.3%	90.9%	84.6%	96.8%	93.4%
2	94.0%	96.0%	88.0%	91.2%	91.7%	93.0%	89.4%	96.1%	80.0%	96.6%	96.3%
3	94.1%	96.2%	92.3%	93.4%	90.8%	83.6%	90.8%	94.9%	97.2%	96.2%	98.4%
4	94.1%	96.2%	95.7%	92.7%	95.1%	88.1%	91.5%	90.9%	89.4%	94.2%	93.3%
5	93.5%	96.8%	83.7%	90.9%	86.8%	88.0%	90.3%	89.3%	88.8%	86.8%	89.9%
6	90.5%	93.9%	76.7%	80.4%	87.0%	75.3%	87.0%	86.0%	94.2%	90.8%	87.3%
7	95.1%	97.9%	88.8%	94.1%	93.6%	90.6%	90.4%	82.1%	79.4%	88.1%	87.2%
8	92.9%	96.6%	89.2%	85.8%	88.9%	81.8%	84.9%	85.1%	86.4%	85.9%	95.8%
mean (std)	93.5% (1.4%)	96.3% (1.1%)	87.8% (5.7%)	90.0% (4.8%)	90.1% (3.1%)	85.3% (5.7%)	89.2% (2.2%)	89.4% (4.8%)	87.5% (6.3%)	91.9% (4.9%)	92.7% (4.2%)

TABLE IV:

Subject-specific classification results. Accuracy refers to the overall success of the algorithm, computed as the number of instances that were correctly classified, divided by the number of all instances. The remaining values refer to the TPR of each movement, computed as the number of instances the specific movement was classified correctly, divided by the number of instances of that movement. Subject 1 is the first author.

sensor was shifted between experiments. In spite of this, inter-subject variation was low, thereby suggesting that accurate and objective classification can be achieved with our system in various settings. Furthermore, inaccuracies are not due to familiarity with the system (or lack thereof), as the algorithm did not perform significantly better with data on the first author's movements, relative to data on other subjects.

Surprisingly, we found that shoulder abduction, shoulder flexion, and vertical rotation were classified with similar accuracy, even though vertical rotation involves shoulder abduction and shoulder flexion to some extent. While one would expect that this movement would be most misclassified, this was not the case, offering further demonstration of the viability of data science-principled approaches in the study of complex processes. Decision trees in particular, are capable of unraveling unique, nonlinear relationships between a feature and a response [52]. Future research could test the efficacy of alternative classifiers such as Support Vector Machines [53], RUSBoot [54], and Subspace K-Nearest Neighbor [55] in classifying bimanual movements.

A possible caveat in our use of PCA is its linear nature, which may prompt the consideration of additional methods to extract features. While literature posits that human motion consists of linearly superimposed motor primitives [56], [57], nonlinear relationships may arise between primitives in bimanual movements and in abnormal, pathological movements in particular. Therefore, under these circumstances, nonlinear dimensionality reduction methods such as Isomap

[58], diffusion maps [59], and principal manifolds [60] may better identify the variables that distinguish one movement from another. Furthermore, features that are based on complexity measures such as fractal dimensions may be more distinctive and informative in assessment of rehabilitation progress, and should be considered [61], [62].

Optimally, our system would solely rely on a Kinect sensor and a dowel, without the need of an IMU sensor. While IMUs are affordable, their incorporation requires customization, which would reduce patients' accessibility to our system. Unfortunately, our analysis of feature importance indicated that measurements of the IMU pitch and yaw were essential in the classification process. To overcome this limitation, in our future efforts we will also explore alternative sets of classifiers and features that are independent of the IMU, and can maintain accuracy in its absence [49]. We may also explore alternative interfaces. For example, strapping a smartphone to the dowel may replace both the Kinect and IMU. Smartphones are embedded with a multitude of sensors, including an IMU, which provide rich and highly sensitive data. In this case, we will test the capacity of features drawn from the sensors embedded in smartphones alone.

The use of the Kinect sensor in our system is central to our proposed paradigm. Being a natural user interface, the Kinect offers great flexibility with respect to the movements that can be implemented in our system. In its current setting, the system aims to improve patients' range of motion through bimanual training. However, one can take advantage of the engaging citizen science software and tailor it to task-oriented rehabilitation exercise [63]. Conceivably, users could control cursor movements by practicing different gross motor skills such as reaching, pulling, and sitting and standing, thereby providing patients the multi-faceted treatment they require.

Finally, the feasibility of our approach must be challenged in a clinical setting. Stroke patients may exhibit movement disorders such as segmentation, spasticity, chorea, and adoption of maladaptive movements [64], [65], [66]. Although studies have shown that the Microsoft Kinect is highly precise [23], it remains unknown whether stroke-related disorders can be automatically detected and characterized. It is possible that more classification algorithms will be required to distinguish between healthy and pathological movements. We are presently conducting tests with patients and will promptly implement our approach.

VII. Conclusion

Ubiquitous home-based rehabilitation is becoming increasingly inevitable. We presented a low-cost telerehabilitation system that can facilitate bimanual exercise in patients' homes. We tested the feasibility of our approach with eight healthy subjects, demonstrating a strong promise toward future studies with both healthy individuals and patients. In the next steps, we will conduct a study with stroke patients to test the proposed approach in a clinical setting. The data presented herein will serve as measures of healthy movement to compare against pathological movements.

The efforts put forth represent a great stride in the field of rehabilitation medicine. First of all, the telerehabilitation system we developed focuses on bimanual training in a home-setting. Although bimanual therapy is effective, it has not been tested in a telerehabilitation paradigm. The system itself is affordable, intuitive to use, and easy to set up by a patient independently at home. Second, the system consists of an interactive and engaging natural user interface. Through this design, we aim to add motive to exercise movements and enhance patients' adherence to their prescribed regimen. Third, a classification algorithm is integrated into the system toward automatic assessment of motor performance. Introducing data science methodologies into human motion analysis could improve accuracy and benefit current medical practices in telerehabiliation where data is acquired without supervision. Although presented here in the context of stroke rehabilitation, the application of our technology is generalizable to other conditions that require rehabilitation. Ultimately, it could accelerate assessment and provide patients with more frequent feedback from a therapist at a lower cost, thereby improving rehabilitation outcomes.

Acknowledgments

This study is part of the collaborative activities carried out under the programs of the region of Murcia (Spain): "Groups of Excellence of the region of Murcia, the Fundacion Seneca, Science and Technology Agency" project 19884/GERM/15 and "Call for Fellowships for Guest Researcher Stays at Universities and OPIS" project 21144/IV/19. The research was supported by the National Science Foundation awards number CBET-1604355 and ECCS-1928614. R.B.V.'s work was supported in part by a Mitsui USA Foundation scholarship. The authors would like to thank Z. Wang for software development and F. V. Surano for valuable input.

Author Contributions

R.B.V., O.N., P.R., and M.P. designed the overall research. O.N., P.R., and M.P. secured the funding. R.B.V. and P.R. designed the experimental system. R.B.V. developed the experimental system and conducted the experiments. R.B.V., M.R.M., and M.P. developed the approach to perform the motion analysis and analyzed the data. R.B.V. wrote a first draft. M.P. supervised the research. All the authors reviewed and approved the final submission.

References

[1] E. C. Leira, A. N. Russman, J. Biller, D. L. Brown, C. D. Bushnell, V. Caso, A. Chamorro, C. J. Creutzfeldt, S. Cruz-Flores, M. S. Elkind *et al.*, "Preserving stroke care during the COVID-19 pandemic: Potential issues and solutions," *Neurology*, 2020.

[2] H. S. Markus and M. Brainin, "COVID-19 and stroke: A global world stroke organization perspective," *International Journal of Stroke*, vol. 15, no. 4, pp. 361–364, 2020.

[3] P. Langhorne, F. Coupar, and A. Pollock, "Motor recovery after stroke: A systematic review," *Lancet Neurology*, vol. 8, no. 8, pp. 741–754, 2009.

[4] B. T. Volpe, D. Lynch, A. Rykman-Berland, M. Ferraro, M. Galgano, N. Hogan, and H. I. Krebs, "Intensive sensorimotor arm training mediated by therapist or robot improves hemiparesis in patients with chronic stroke," *Neurorehabilitation and Neural Repair*, vol. 22, no. 3, pp. 305–310, 2008.

[5] B. H. Dobkin, "Rehabilitation after stroke," *New England Journal of Medicine*, vol. 352, no. 16, pp. 1677–1684, 2005.

[6] C. E. Skilbeck, D. T. Wade, R. L. Hewer, and V. A. Wood, "Recovery after stroke," *Journal of Neurology, Neurosurgery and Psychiatry*, vol. 46, no. 1, pp. 5–8, 1983.

[7] M. Eriksson, B. Norrving, A. Terént, and B. Stegmayr, "Functional outcome 3 months after stroke predicts long-term survival," *Cerebrovascular Diseases*, vol. 25, no. 5, pp. 423–429, 2008.

[8] M. J. Rosen, "Telerehabilitation," *NeuroRehabilitation*, vol. 12, no. 1, pp. 11–26, 1999.

[9] M. Rogante, M. Grigioni, D. Cordella, and C. Giacomozzi, "Ten years of telerehabilitation: A literature overview of technologies and clinical applications," *NeuroRehabilitation*, vol. 27, no. 4, pp. 287–304, 2010.

[10] D. J. Reinkensmeyer, C. T. Pang, J. A. Nessler, and C. C. Painter, "Web-based telerehabilitation for the upper extremity after stroke," *IEEE Transactions on Neural Systems and Rehabilitation Engineering*, vol. 10, no. 2, pp. 102–108, 2002.

[11] C. R. Carignan and H. I. Krebs, "Telerehabilitation robotics: Bright lights, big future?" *Journal of Rehabilitation Research and Development*, vol. 43, no. 5, p. 695, 2006.

[12] H. I. Krebs, B. T. Volpe, D. Williams, J. Celestino, S. K. Charles, D. Lynch, and N. Hogan, "Robot-aided neurorehabilitation: A robot for wrist rehabilitation," *IEEE Transactions on Neural Systems and Rehabilitation Engineering*, vol. 15, no. 3, pp. 327–335, 2007.

[13] L. Masia, H. I. Krebs, P. Cappa, and N. Hogan, "Design and characterization of hand module for whole-arm rehabilitation following stroke," *IEEE/ASME Transactions on Mechatronics*, vol. 12, no. 4, pp. 399–407, 2007.

[14] D. M. Brennan, P. S. Lum, G. Uswatte, E. Taub, B. M. Gilmore, and J. Barman, "A telerehabilitation platform for home-based automated therapy of arm function," in *2011 Annual International Conference of the IEEE Engineering in Medicine and Biology Society*. IEEE, 2011, pp. 1819–1822.

[15] C.-y. Wu, C.-l. Yang, K.-c. Lin, L.-l. Wu *et al.*, "Unilateral versus bilateral robot-assisted rehabilitation on arm-trunk control and functions post stroke: a randomized controlled trial," *Journal of Neuroengineering and Rehabilitation*, vol. 10, no. 1, p. 35, 2013.

[16] P. Raghavan, V. Aluru, S. Milani, P. Thai, D. Geller, S. Bilaloglu, Y. Lu, and D. J. Weisz, "Coupled bimanual training using a non-powered device for individuals with severe hemiparesis: a pilot study," *International Journal of Physical Medicine and Rehabilitation*, vol. 5, no. 3, 2017.

[17] S. Lum, S. L. Lehman, and D. J. Reinkensmeyer, "The bimanual lifting rehabilitator: An adaptive machine for therapy of stroke patients," *IEEE Transactions on Rehabilitation Engineering*, vol. 3, no. 2, pp. 166–174, 1995.

[18] N. Wenderoth, F. Debaere, S. Sunaert, P. v. Hecke, and S. P. Swinnen, "Parieto-premotor areas mediate directional interference during bimanual movements," *Cerebral Cortex*, vol. 14, no. 10, pp. 1153–1163, 2004.

[19] K. C. Stewart, J. H. Cauraugh, and J. J. Summers, "Bilateral movement training and stroke rehabilitation: A systematic review and meta-analysis," *Journal of the Neurological Sciences*, vol. 244, no. 1-2, pp. 89–95, 2006.

[20] S. P. Swinnen and N. Wenderoth, "Two hands, one brain: Cognitive neuroscience of bimanual skill," *Trends in Cognitive Sciences*, vol. 8, no. 1, pp. 18–25, 2004.

[21] J. Shotton, T. Sharp, A. Kipman, A. Fitzgibbon, M. Finocchio, A. Blake, M. Cook, and R. Moore, "Real-time human pose recognition in parts from single depth images," *Communications of the ACM*, vol. 56, no. 1, pp. 116–124, 2013.

[22] Z. Zhang, "Microsoft Kinect sensor and its effect," *IEEE Multimedia*, vol. 19, no. 2, pp. 4–10, 2012.

[23] A. Fern'ndez-Baena, A. Susín, and X. Lligadas, "Biomechanical validation of upper-body and lower-body joint movements of Kinect motion capture data for rehabilitation treatments," in *IEEE 4th International Conference on Intelligent Networking and Collaborative Systems*. IEEE, 2012, pp. 656–661.

[24] J. W. Burke, M. McNeill, D. K. Charles, P. J. Morrow, J. H. Crosbie, and S. M. McDonough, "Optimising engagement for stroke rehabilitation using serious games," *The Visual Computer*, vol. 25, no. 12, p. 1085, 2009.

[25] E. Flores, G. Tobon, E. Cavallaro, F. I. Cavallaro, J. C. Perry, and T. Keller, "Improving patient motivation in game development for motor deficit rehabilitation," in *Proceedings of the International Conference on Advances in Computer Entertainment Ttechnology*, 2008, pp. 381–384.

[26] V. M. Conraads, C. Deaton, E. Piotrowicz, N. Santaularia, S. Tierney, M. F. Piepoli, B. Pieske, J.-P. Schmid, K. Dickstein, P. P. Ponikowski *et al.*, "Adherence of heart failure patients to exercise: barriers and possible solutions: a position statement of the study group on exercise training in heart failure of the heart failure association of the european society of cardiology," *European Journal of Heart Failure*, vol. 14, no. 5, pp. 451–458, 2012.

[27] J. Laut, F. Cappa, O. Nov, and M. Porfiri, "Increasing patient engagement in rehabilitation exercises using computer-based citizen science," *PLOS ONE*, vol. 10, no. 3, p. e0117013, 2015.

[28] R. B. Ventura, S. Nakayama, P. Raghavan, O. Nov, and M. Porfiri, "The role of social interactions in motor performance: Feasibility study toward enhanced motivation in telerehabilitation," *Journal of Medical Internet Research*, vol. 21, no. 5, p. e12708, 2019.

[29] S. H. Holzreiter and M. E. Köhle, "Assessment of gait patterns using neural networks," *Journal of Biomechanics*, vol. 26, no. 6, pp. 645–651, 1993.

[30] M. J. O'Malley, M. F. Abel, D. L. Damiano, and C. L. Vaughan, "Fuzzy clustering of children with cerebral palsy based on temporal-distance gait parameters," *IEEE Transactions on Rehabilitation Engineering*, vol. 5, no. 4, pp. 300–309, 1997.

[31] N. Abaid, P. Cappa, E. Palermo, M. Petrarca, and M. Porfiri, "Gait detection in children with and without hemiplegia using single-axis wearable gyroscopes," *PLOS ONE*, vol. 8, no. 9, p. e73152, 2013.

[32] J. Taborri, S. Rossi, E. Palermo, F. Patanè, and P. Cappa, "A novel hmm distributed classifier for the detection of gait phases by means of a wearable inertial sensor network," *Sensors*, vol. 14, no. 9, pp. 16 212–16 234, 2014.

[33] A. Mannini, D. Trojaniello, A. Cereatti, and A. M. Sabatini, "A machine learning framework for gait classification using inertial sensors: Application to elderly, post-stroke and huntington's disease patients," *Sensors*, vol. 16, no. 1, p. 134, 2016.

[34] R. Begg and J. Kamruzzaman, "A machine learning approach for automated recognition of movement patterns using basic, kinetic and kinematic gait data," *Journal of Biomechanics*, vol. 38, no. 3, pp. 401–408, 2005.

[35] D. Novak, P. Reberšek, S. M. M. De Rossi, M. Donati, J. Podobnik, T. Beravs, T. Lenzi, N. Vitiello, M. C. Carrozza, and M. Munih, "Automated detection of gait initiation and termination using wearable sensors," *Medical Engineering and Physics*, vol. 35, no. 12, pp. 1713–1720, 2013.

[36] E. V. Olesh, S. Yakovenko, and V. Gritsenko, "Automated assessment of upper extremity movement impairment due to stroke," *PLOS ONE*, vol. 9, no. 8, p. e104487, 2014.

[37] K. Ongvisatepaiboon, J. H. Chan, and V. Vanijja, "Smartphone-based tele-rehabilitation system for frozen shoulder using a machine learning approach," in *2015 IEEE Symposium Series on Computational Intelligence*. IEEE, 2015, pp. 811–815.

[38] A. Rajkumar, F. Vulpi, S. Reddy Beth, P. Raghavan, and V. Kapila, "Usability study of wearable inertial sensors for exergames (wise) for movement assessment and exercise," *mHealth*, 2020.

[39] M. Huber, A. L. Seitz, M. Leeser, and D. Sternad, "Validity and reliability of kinect skeleton for measuring shoulder joint angles: A feasibility study," *Physiotherapy*, vol. 101, no. 4, pp. 389–393, 2015.

[40] S. Moon, Y. Park, D. W. Ko, and I. H. Suh, "Multiple Kinect sensor fusion for human skeleton tracking using Kalman filtering," *International Journal of Advanced Robotic Systems*, vol. 13, no. 2, p. 65, 2016.

[41] S. M. Hatem, G. Saussez, M. della Faille, V. Prist, X. Zhang, D. Dispa, and Y. Bleyenheuft, "Rehabilitation of motor function after stroke: a multiple systematic review focused on techniques to stimulate upper extremity recovery," *Frontiers in Human Neuroscience*, vol. 10, p. 442, 2016.

[42] S. B. Thompson and M. Morgan, *Occupational therapy for stroke rehabilitation*. Springer, 2013.

[43] L. Oujamaa, I. Relave, J. Froger, D. Mottet, and J.-Y. Pelissier, "Rehabilitation of arm function after stroke: Literature review," *Annals of Physical and Rehabilitation Medicine*, vol. 52, no. 3, pp. 269–293, 2009.

[44] S. L. Wolf, D. E. Lecraw, L. A. Barton, and B. B. Jann, "Forced use of hemiplegic upper extremities to reverse the effect of learned nonuse among chronic stroke and head-injured patients," *Experimental Neurology*, vol. 104, no. 2, pp. 125–132, 1989.

[45] D. Lynch, M. Ferraro, J. Krol, C. M. Trudell, P. Christos, and B. T. Volpe, "Continuous passive motion improves shoulder joint integrity following stroke," *Clinical Rehabilitation*, vol. 19, no. 6, pp. 594–599, 2005.

[46] P. Raghavan, Y. Lu, M. Mirchandani, and A. Stecco, "Human recombinant hyaluronidase injections for upper limb muscle stiffness in individuals with cerebral injury: a case series," *EBioMedicine*, vol. 9, pp. 306–313, 2016.

[47] E. Palermo, J. Laut, O. Nov, P. Cappa, and M. Porfiri, "A natural user interface to integrate citizen science and physical exercise," *PLOS ONE*, vol. 12, no. 2, p. e0172587, 2017.

[48] A. Pacilli, M. Germanotta, S. Rossi, and P. Cappa, "Quantification of age-related differences in reaching and circle-drawing using a robotic rehabilitation device," *Applied Bionics and Biomechanics*, vol. 11, no. 3, pp. 91–104, 2014.

[49] N. Murrell, R. Bradley, N. Bajaj, J. G. Whitney, and G. T.-C. Chiu, "A method for sensor reduction in a supervised machine learning classification system," *IEEE/ASME Transactions on Mechatronics*, vol. 24, no. 1, pp. 197–206, 2018.

[50] T. G. Dietterich, "An experimental comparison of three methods for constructing ensembles of decision trees: Bagging, boosting, and randomization," *Machine Learning*, vol. 40, no. 2, pp. 139–157, 2000.

[51] A. M. Prasad, L. R. Iverson, and A. Liaw, "Newer classification and regression tree techniques: Bagging and random forests for ecological prediction," *Ecosystems*, vol. 9, no. 2, pp. 181–199, 2006.

[52] S. Shalev-Shwartz and S. Ben-David, *Understanding machine learning: From theory to algorithms*. Cambridge University Press, 2014.

[53] W. S. Noble, "What is a support vector machine?" *Nature Biotechnology*, vol. 24, no. 12, pp. 1565–1567, 2006.

[54] C. Seiffert, T. M. Khoshgoftaar, J. Van Hulse, and A. Napolitano, "Rusboost: A hybrid approach to alleviating class imbalance," *IEEE Transactions on Systems, Man, and Cybernetics-Part A: Systems and Humans*, vol. 40, no. 1, pp. 185–197, 2009.

[55] S. Sun and C. Zhang, "Subspace ensembles for classification," *Physica A: Statistical Mechanics and its Applications*, vol. 385, no. 1, pp. 199–207, 2007.

[56] T. Flash and B. Hochner, "Motor primitives in vertebrates and invertebrates," *Current Opinion in Neurobiology*, vol. 15, no. 6, pp. 660–666, 2005.

[57] X. Ding and C. Fang, "A novel method of motion planning for an anthropomorphic arm based on movement primitives," *IEEE/ASME Transactions on Mechatronics*, vol. 18, no. 2, pp. 624–636, 2012.

[58] J. B. Tenenbaum, V. De Silva, and J. C. Langford, "A global geometric framework for nonlinear dimensionality reduction," *Science*, vol. 290, no. 5500, pp. 2319–2323, 2000.

[59] R. R. Coifman, S. Lafon, A. B. Lee, M. Maggioni, B. Nadler, F. Warner, and S. W. Zucker, "Geometric diffusions as a tool for harmonic analysis and structure definition of data: Diffusion maps," *Proceedings of the National Academy of Sciences*, vol. 102, no. 21, pp. 7426–7431, 2005.

[60] K. Gajamannage, S. Butail, M. Porfiri, and E. M. Bollt, "Dimensionality reduction of collective motion by principal manifolds," *Physica D: Nonlinear Phenomena*, vol. 291, pp. 62–73, 2015.

[61] Y. Zou, R. V. Donner, N. Marwan, J. F. Donges, and J. Kurths, "Complex network approaches to nonlinear time series analysis," *Physics Reports*, vol. 787, pp. 1–97, 2019.

[62] A. Phinyomark, R. Larracy, and E. Scheme, "Fractal analysis of human gait variability via stride interval time series," *Frontiers in Physiology*, vol. 11, p. 333, 2020.

[63] M. Rensink, M. Schuurmans, E. Lindeman, and T. Hafsteinsdottir, "Task-oriented training in rehabilitation after stroke: systematic review," *Journal of Advanced Nursing*, vol. 65, no. 4, pp. 737–754, 2009.

[64] F. Alarcon, J. Zijlmans, G. Duenas, and N. Cevallos, "Post-stroke movement disorders: report of 56 patients," *Journal of Neurology, Neurosurgery and Psychiatry*, vol. 75, no. 11, pp. 1568–1574, 2004.

[65] A. Handley, P. Medcalf, K. Hellier, and D. Dutta, "Movement disorders after stroke," *Age and Ageing*, vol. 38, no. 3, pp. 260–266, 2009.

[66] N. Takeuchi and S.-I. Izumi, "Maladaptive plasticity for motor recovery after stroke: mechanisms and approaches," *Neural Plasticity*, vol. 2012, 2012.

Roni Barak-Ventura Roni Barak Ventura received B.Sc. degree in Evolutionary Biology and Ecology from the University of Rochester in 2014, and M.Sc. degree in Biomedical Engineering from New York University Tandon School of Engineering in 2017. She is currently pursuing a Ph.D degree at New York University Tandon School of Engineering under the guidance of Professor Maurizio Porfiri. Her research interests include rehabilitation, human-computer interaction, and dynamical systems.

Manuel Ruiz-Marín Dr. Manuel Ruiz-Marín is a Professor at the Technical University of Cartagena in the Department of Quantitative Methods and Murcia Bio-Health Institute (IMIB-Arrixaca). He obtained his M.Sc. and Ph.D. degrees in Mathematics from the University of Murcia, Spain. He was granted a post-doctoral fellowship at Free University of Brussels. Ruiz-Marín's main research interests involve complex BigData of Spatial and Time processes, including the study of spatial statistics econometrics, non-parametric statistics, symbolic analysis, and complex networks. He has more than 80 scientific publications in outstanding international journals, having participated in more than 16 research projects (several of them as principal investigator) with national and international teams. He is currently the Principal Investigator of the Excellence Research Group (EMODs) from Séneca Fundation.

Oded Nov Oded Nov is a Professor at New York University's Tandon School of Engineering. He received his PhD at Cambridge University, and his research focuses on social computing, human-computer interaction, and the future of expert work in healthcare. Nov is a recipient of the U.S. National Science Foundation CAREER Award, and his research is supported by the National Science Foundation, the National Academies Keck Initiative, the MacArthur Foundation, and Google.

Preeti Raghavan Preeti Raghavan received her M.D. from the Rajah Muthiah Medical College in India in 1997 and completed her residency in Physical Medicine and Rehabilitation from the Albert Einstein College of Medicine, Bronx, NY, USA, in 2002. She is currently the Sheikh Khalifa Stroke Institute Endowed Chair and the Director of the Center of Excellence for Treatment, Recovery and Rehabilitation in the departments of Physical Medicine and Rehabilitation and Neurology at the Johns Hopkins University School of Medicine. She is also an adjunct associate professor at Rusk Rehabilitation, New York University School of Medicine. Her research interests are in motor control, rehabilitation engineering, and stroke rehabilitation.

Maurizio Porfiri Dr. Maurizio Porfiri is an Institute Professor at NYU Tandon School of Engineering, with appointments in the Center for Urban Science and Progress and the Departments of Mechanical and Aerospace Engineering, Biomedical Engineering, and Civil and Urban Engineering. He received M.Sc. and Ph.D. degrees in Engineering Mechanics from Virginia Tech, in 2000 and 2006; a "Laurea" in Electrical Engineering (with honors) and a Ph.D. in Theoretical and Applied Mechanics from the University of Rome "La Sapienza" and the University of Toulon (dual degree program), in 2001 and 2005, respectively. He has been on the faculty of the Mechanical and Aerospace Engineering Department since 2006, when he founded the Dynamical Systems Laboratory. Dr. Porfiri is a Fellow of the American Society of Mechanical Engineers (ASME) and the Institute of Electrical and Electronic Engineers (IEEE). He has served in the Editorial Board of ASME Journal of Dynamics systems, Measurements and Control, ASME Journal of Vibrations and Acoustics, Flow, IEEE Control Systems Letters, IEEE Transactions on Circuits and Systems I, and Mechatronics. Dr. Porfiri is engaged in conducting and supervising research on dynamical systems theory, multi-physics modeling, and underwater robotics. He is the author of more than 350 journal publications and the recipient of the National Science Foundation CAREER award. He has been included in the "Brilliant 10" list of Popular Science in 2010 and his research featured in all the major media outlets, including CNN, NPR, Scientific American, and Discovery Channel. Other significant recognitions include invitations to the Frontiers of Engineering Symposium and the Japan-America Frontiers of Engineering Symposium organized by National Academy of Engineering; the Outstanding Young Alumnus award by the college of Engineering of Virginia Tech; the ASME Gary Anderson Early Achievement Award; the ASME DSCD Young Investigator Award; and the ASME C.D. Mote, Jr. Early Career Award.